American Meteorological Society
11th Conference on Mountain Meteorology
21-25 June 2004, Bartlett NH

8.6

DIURNAL CYCLES OF THERMALLY DRIVEN FLOWS IN TWO ADJACENT UTAH VALLEY SYSTEMS AS REVEALED BY EOF FLOW PATTERNS

F. L. Ludwig, Stanford University, John Horel, University of Utah and
C. David Whiteman, Pacific Northwest National Laboratory

1. Introduction

Empirical Orthogonal Function (EOF) methods can reveal data patterns and their diurnal variations so that the underlying physical processes are apparent. They can also reduce the number of parameters required to define simultaneous behavior at several locations. Here, the technique revealed major flow patterns and their diurnal cycles for thermally driven flows with weak synoptic forcing in the Great Salt Lake area of Utah.

2. Study area and data

2.1 Salt Lake and Rush Valley areas

Figure 1 shows the study area and meteorological site locations used. Altitudes range from 1270 m (Great Salt Lake) to over 3000 m in the Wasatch and Oquirrh Mountains. The latter range separates the Salt Lake/Utah Valleys from the Rush/Tooele Valleys to the west. The Salt Lake Valley is separated from the Utah Lake Valley by the Traverse Mountains through which the Jordan River passes. at the Jordan Narrows. The Rush and Tooele Valleys are separated by an east-west ridge called South Mountain, (unmarked in Figure 1).

Stewart et al. (2002) noted that the parallel valley systems, the two lakes and the many side canyons drive diurnal cycles of lake-land breezes and slope-valley flows, especially under weak synoptic influences, when surface winds decouple from synoptic flow at night, causing gravity flows to develop, often reinforced by land breezes. Conditions reverse during the day when surfaces are heated. During morning transitions, the lake breeze penetrates into the Tooele Valley before it develops in the Salt Lake Valley. Flows up the valley and up its sidewalls and canyons all interact with the lake breezes In the afternoon (Stewart et al. 2002).

2.2 Data sources and selection

The analyses here were motivated by those of Ludwig et al. (2002), using special data from the Vertical Transport and Mixing eXperiment (VTMX) in the Salt Lake Valley (Doran et al. 2002), and by Stewart et al. (2002), who used data from the MesoWest archive (Horel et al. 2002) for thermally driven summer flows in 1997 through 2000 with "clear to partly cloudy" skies (as defined by Whiteman et al. 1999) and 700-hPa winds less than 7 m s^{-1}. We used a subset of the MesoWest data collected by Stewart et al. (2002) and VTMX data.

Sets of eight MesoWest stations each in the Tooele/Rush and the Salt Lake/Utah Lake Valleys were selected to represent axial and side slope flows, as well as at side canyon entrances, where possible. Trial and error maximized the numbers of available cases in each valley, while still retaining locations that would represent important flow features. The station selection procedure is described more completely by Ludwig et al. (2004). Station locations for the data sets are shown in Figure 1. There were 2281 hours from the Tooele/Rush Valleys, and 1399 from the Utah/Salt Lake Valleys.

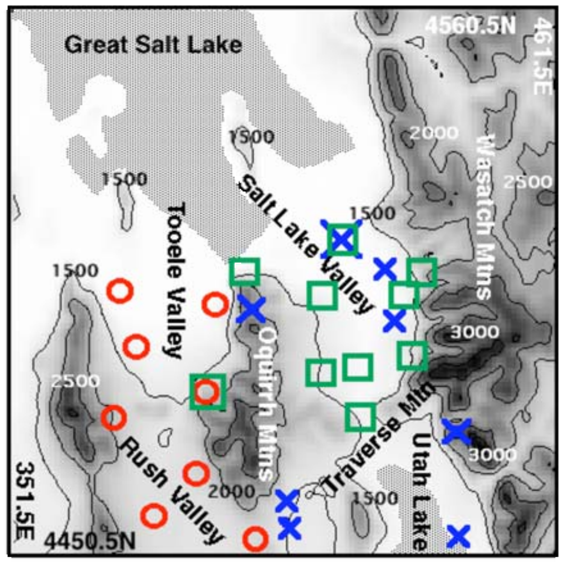

FIGURE 1 TOOELE/RUSH (O), SALT/UTAH LAKE (X) AND VTMX CAMPAIGN (□) WIND OBSERVATION SITES

VTMX data were used differently; they were objectively analyzed with the Winds on Critical Streamline Surfaces (WOCSS, Ludwig et al. 1991) diagnostic model. It defines surfaces on which the flow takes place; in stable atmospheres, the surfaces reach a maximum height determined by the lapse rate and the wind's kinetic energy. Winds interpolated to the surfaces are iteratively adjusted toward two-dimensional non-divergence thereby forcing flow around any terrain obstacles that intersect the surfaces. Winds at grid points near selected observation sites were chosen for EOF analysis in order to provide complete data sets from all selected locations for every half hour for ten VTMX intensive operating periods (IOPs). No case had to be eliminated because of a missing observation. This is important because the EOF analysis works best with a large number of complete data sets; 454 half-hourly cases were available for analysis from the ten VTMX IOPs.

3. EOF analysis methodology

EOFs have been widely used to reveal physically important connections in meteorological and climatological studies ever since Lorenz (1956) used them to represent U.S. pressure and temperature fields and reduce the number of predictors required for statistical forecasting. The method works best when physical processes produce well defined flow patterns. Stewart et al. (2002) had earlier found well organized flows in the Tooele and Salt Lake valleys, so we expected that EOFs would provide useful information in this area.

Lorenz studied scalar fields, but vector fields can also be analyzed (e.g. Lumley 1981; Hardy 1977; Ludwig and Byrd 1980). Kaihatu et al. (1998) describe advantages and disadvantages in representing vectors as complex numbers versus scalar pairs (or triplets for 3-d vectors). We chose to use scalar pairs of u and v components. EOF determination is relatively standard; Lorenz's (1956) classic report describes the details of the method (see also, von Storch and Zwiers 1999; Wilks 1995). For our purposes, it is enough to note that the objective is to reduce the number of variables required to describe the data, while losing the least possible information. For winds collected at N locations at time t, the data can be represented as:

$$\begin{pmatrix} u_1(t) \\ v_1(t) \\ u_2(t) \\ v_2(t) \\ \bullet \\ \bullet \\ \bullet \\ u_N(t) \\ v_N(t) \end{pmatrix} = \begin{pmatrix} \bar{u}_1 \\ \bar{v}_1 \\ \bar{u}_2 \\ \bar{v}_2 \\ \bullet \\ \bullet \\ \bullet \\ \bar{u}_N \\ \bar{v}_N \end{pmatrix} + \sum_{i=1}^{2N} a_i(t) \begin{pmatrix} u_{1,i} \\ v_{1,i} \\ u_{2,i} \\ v_{2,i} \\ \bullet \\ \bullet \\ \bullet \\ u_{N,i} \\ v_{N,i} \end{pmatrix} \qquad (1)$$

The left hand side (LHS) column vector in Equation 1 represents observed u and v components for time t at N sites; subscripts denote different sites. The first right hand side (RHS) vector contains u and v component means for the complete data set, that is, the averages derived from all the available observations at the N sites. The remaining RHS terms have scalar coefficients $a_i(t)$ that vary with time. A few of these scalar terms and their associated vectors usually describe the data quite well. The column vectors that are multiplied by the scalars are the EOFs that we will discuss. The EOFs have the following attributes: 1) they are unit vectors (normalized eigenvectors of a matrix related to the covariance matrix), 2) they are arranged in decreasing order of explained variance, and 3) they are orthogonal (uncorrelated). At a time t, the i^{th} EOF coefficient, $a_i(t)$, is the inner product of the i^{th} EOF and the observation vector (LHS) minus the mean.

With RHS terms in order of descending importance (explained variance), the first few terms generally estimate the wind field well. Agreement between observations and estimates improves with added terms, but the effects are usually small after the first two or three terms. For well correlated data (e. g., winds governed by strong physical processes), one EOF can explain more than 50% of the variance, equivalent to a correlation of greater than 0.7 between estimates and observations.

EOFs can be displayed graphically to make patterns evident. Observed winds, which are the elements in the LHS column vector of Equation 1, can be plotted as vectors on a map. So too can the RHS averages and each of the EOFs, EOFs do not necessarily reflect a specific physical process, but strong processes are likely to be reflected in the first few EOFs, so their coefficients will represent the intensity of certain patterns and the associated physical processes.

4. Results

4.1 Averages

Figure 2 shows averages for the three data sets. Tooele Valley (red arrows) has downslope means at its 6 southern stations, but the two northern sites have means that show that the daytime lake breezes are not offset by the weaker nighttime land breezes. Salt Lake Valley means (blue) have net downslope and down-valley flow, as do the VTMX data (green). Average speeds are all less than 2 m s^{-1}, but the means are biased toward the clear, light wind conditions selected for analysis.

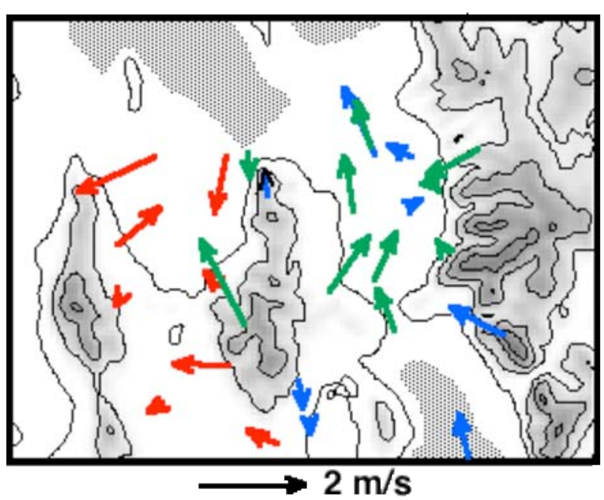

FIGURE 2 MEAN WINDS FOR **TOOELE**, **SALT LAKE** AND **VTMX CAMPAIGN** DATA

4.2 EOFs explaining the most variance

The EOFs explaining the most variance are shown in Figure 3. Nearly half, 47 percent, of the Tooele/Rush Valley variance is accounted for by the first EOF (Figure 3A, red vectors), equivalent to a correlation of nearly 0.7 between observed components (LHS in Equation 1) and values estimated from the mean and first EOF. EOF 2 (Fig 3B, red arrows) explained only 16 percent of the variance in the observations from the Tooele/Rush Valley sites.

EOF 1 (Figure 3A, red) is well organized. All directions align well with valley axes, indicating that channeling and thermally driven along-valley flows dominate. Positive (or negative) EOF 1 coefficients describe down-valley (or up-valley) flow. EOF 2 is orthogonal to EOF 1, so it is no surprise that EOF 2 (Figure 3B, red) defines an out-of-phase relationship between the Toole and Rush Valley winds, as occurs during transitions when the land breeze changes to a lake breeze while nighttime, downslope flow still persists. When the EOF's coefficients are of opposite sign, the northern valley is dominated by lake (– EOF 1 and + EOF 2) or land breezes (+ EOF 1 and – EOF 2).

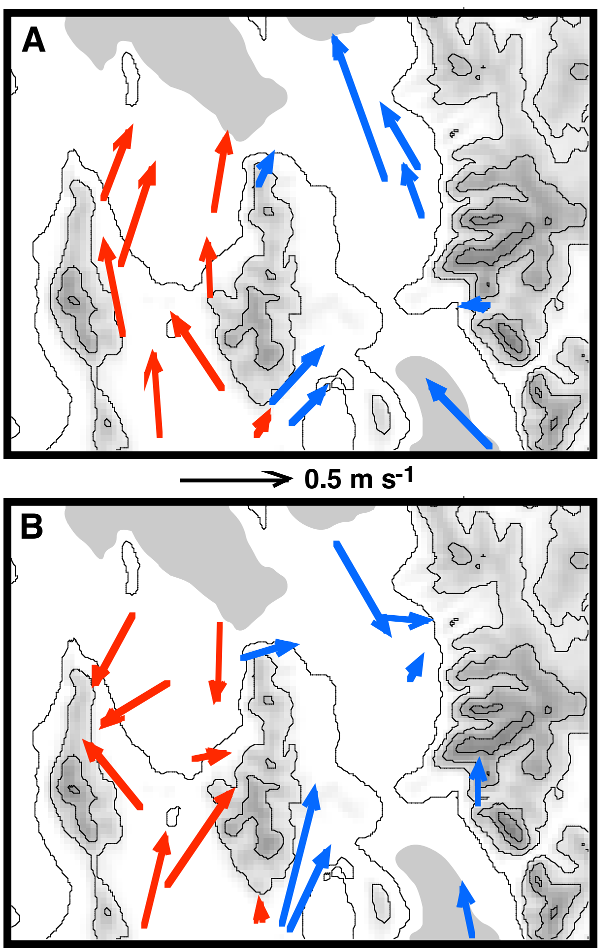

FIGURE 3 EOF 1 (A) AND EOF 2 (B) FOR **TOOELE**, AND **SALT LAKE** DATA

EOF 1 for the Utah/Salt Lake Valleys (Fig. 3A, blue arrows), also reflects the channeling and thermal flows parallel to valley axes. EOF 2 represents oppositely directed flows in the northern and southern regions (Fig 4B, blue); positive EOF 2 coefficients (where contributions are in the directions shown) produce a lake breeze and upslope flows at northern locations, while southern sites have greater downslope components. Negative coefficients will reverse the contribution of the EOF.

EOFs 1 (Figure 4, green arrows) and 2 (pink) from VTMX 2000 observations have greater explained variance than for the other two examples shown in Figure 3, because the area covered is more compact. Again, EOF 1 (Figure 4, green) has an along-valley pattern. EOF 2 (Figure 4, pink) is more complex than those discussed earlier, in part because of the locations of wind sites near canyon mouths and along the broad west slope of the Salt Lake Valley. Those sites introduce more evidence of canyon drainage and slope flow than was possible from the sites in the other data sets.

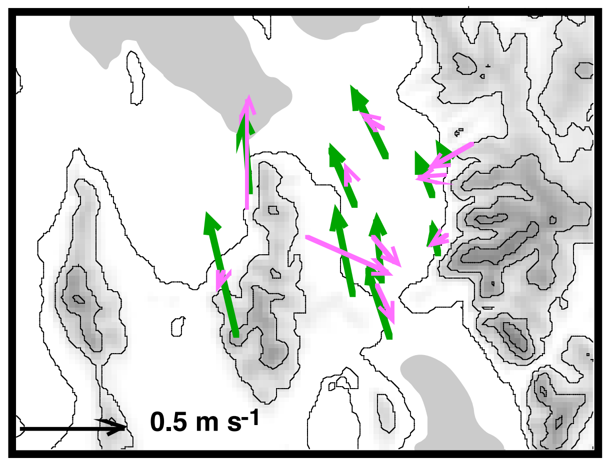

FIGURE 4 **EOF 1** AND **EOF 2** FOR VTMX DATA

4.3 Temporal variability

If the EOFs represent patterns of flow driven by diurnal heating, then the EOF coefficients should have pronounced diurnal cycles. Hourly box plots (prepared with Data Desk 6.0 software, Velleman 1997) in Figure 5 show these diurnal tendencies. The rectangle ("box") in each plot spans values between the lower and upper quartiles; a horizontal line in the box marks the median for that hour. Velleman (1997) states, "The whiskers extend from the top and the bottom of the box to depict the extent of the main body of the data." The small circles and asterisks mark individual outlier values. Each box plot in Figures 5A and 5B represents about 95 values for the Tooele/Rush Valley hours, and about 60 Utah/Salt Lake Valley hours. There is some variation in number of cases from hour to hour.

Diurnal EOF 1 coefficient trends (Fig 5A) in the Tooele/Rush Valley data are obvious, with positive medians between about 2100 and 0900 LST, and negative medians for most daytime hours. Reference to Figure 3A shows this to correspond to the expected cycle for a thermally driven flow, i. e. increased down-valley nighttime winds and up-valley daytime winds. Coefficients are most consistent at night, when low level stability decouples surface winds from the more variable synoptic scale winds aloft. Daytime variability is greater, with the greatest variability occurring during transition periods.

From about midnight until 1000, the medians for EOF2 coefficients (Figure 5B) in the Tooele/Rush Valley are near zero, becoming modestly positive from about 1000 until 1400, with the onset of a lake breeze and continuing drainage from Rush Valley. EOF2 coefficient medians are moderately negative from about 1800 until midnight, during the transition from lake to land breeze. The convective part of the day has the greatest EOF 2 coefficient spread.

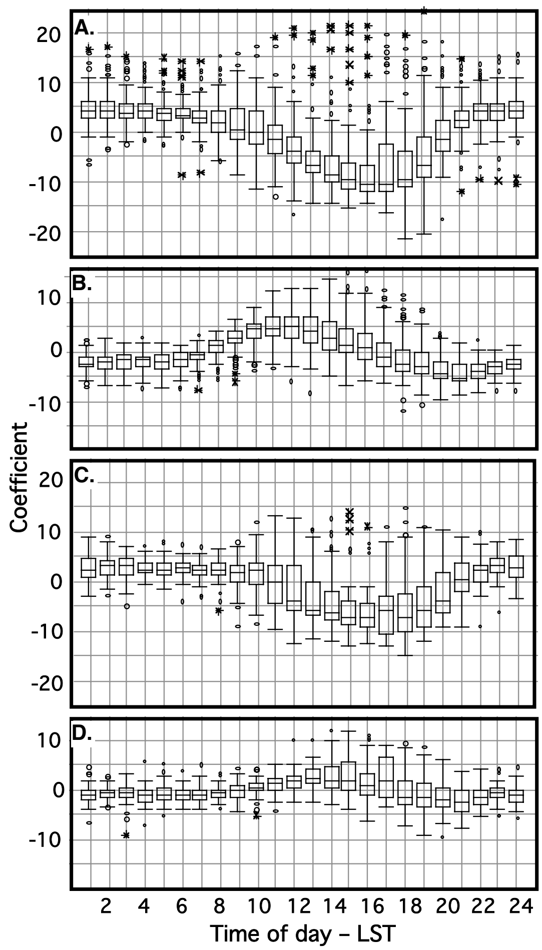

FIGURE 5 DIURNAL COEFFICIENT BOXPLOTS FOR: TOOELE/RUSH VALLEYS: (A) EOF 1, (B) EOF 2, AND SALT LAKE/UTAH LAKE VALLEYS: (C) EOF 1 AND (D) EOF 2,

Utah/Salt Lake Valley EOF 1 diurnal patterns (Figure 5C) are similar to those in Figure 5A, with up-valley/upslope flows (negative EOF 1 coefficients) beginning about noon and lasting past 2000. Positive medians mark the reverse flow at night. They are of smaller magnitude, but have less scatter than in the Tooele/Rush valleys. Utah/Salt Lake Valley EOF 2 median coefficients (Figure 5D) differ significantly from zero only from about 1100 to 1700 LST, when they are positive, and 1800 to 2200, when they are negative. In the Tooele/Rush valleys (Figure 5B), the non-zero periods were associated with morning and evening transitions. EOF 2 in these valleys predominantly represents lake/land breezes in the north. North-northeasterly flow through the pass begins with the lake breeze in the late morning, and reverses when the land breeze starts shortly after sunset.

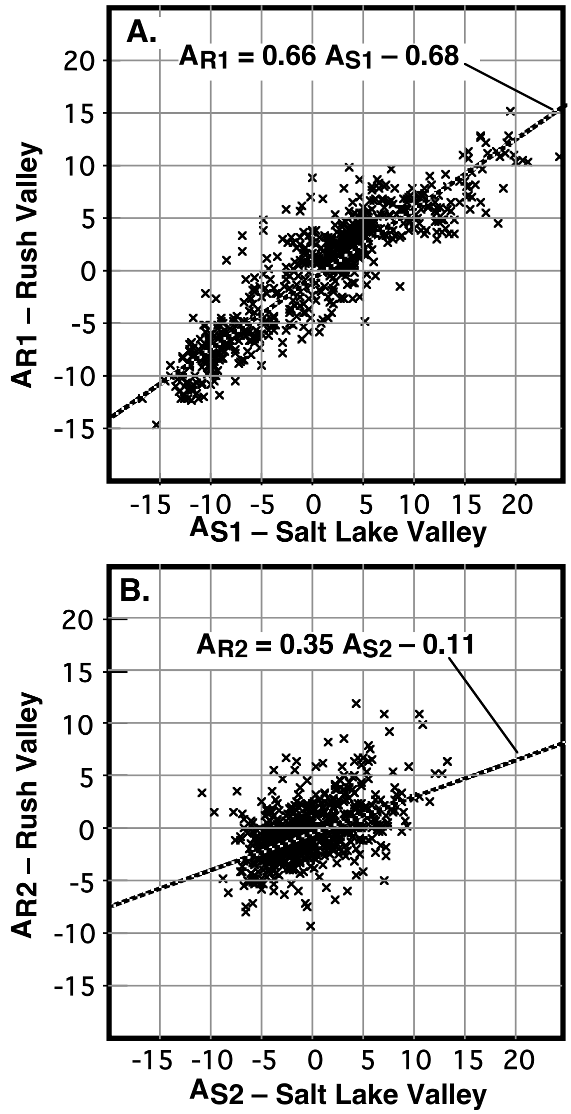

FIGURE 6 COEFFICIENT SCATTERGRAMS AND REGRESSION LINES IN TWO VALLEY SYSTEMS: (A) EOF 1 AND (B) EOF 2

Coefficients for the first EOFs for the two valley systems (Figures 5A and 5C) have similar diurnal cycles and probably represent similar physical processes. Figure 6A is a scatter plot between EOF 1 coefficients from the two valleys for the 765 hours when complete data sets were available in each. Their correlation coefficient r is 0.91. EOF 2 explains much less variance than EOF 1, and the physical processes represented by the second EOFs seem to be different in the two valleys, so it is not surprising that the EOF 2 coefficients in Figure 6B have only a correlation of 0.51.

The coefficient cycle for VTMX 2000 data is shown in Figure 7. Note that the time span in this figure runs from noon to noon, rather than from midnight to midnight as in Figure 5. Each box plot represents about 20 observations, generally for times 15 minutes before and 15 minutes after the hour. Observations on either side of the hour have been assigned to the hour between them.

Temporal changes of the EOF 1 coefficient medians are much the same as in Figures 5A and 5C. Slightly positive medians, corresponding to down-valley winds from the south-southeast, persist from about midnight through noon. Then coefficients become negative (up-valley winds) and continue so until about 2000 LST. Greatest day-to-day variability is between about 0900 and 1500 LST. The sudden reduction in variability from 1500 to 1600 LST indicates that up-valley flow was well established at 1600 LST in most cases. The majority of the outliers in Figure 6A occurred during a single IOP; these will be discussed in the next section.

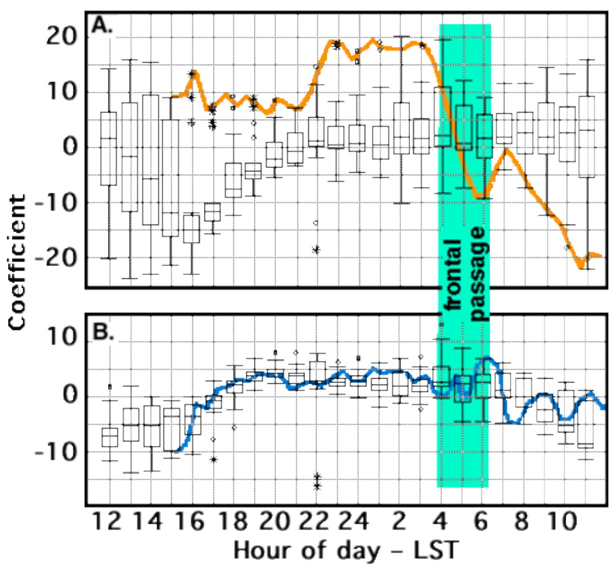

FIGURE 7 DIURNAL COEFFICIENT BOXPLOTS FOR: (A) EOF 1 AND (B) EOF 2, Orange and blue lines show coefficient values for 20-21 October 2000.

EOF 2 coefficient medians in Figure 7B have a similar diurnal cycle to that in Figure 5D, although there are significant differences in the EOFs themselves (Figures 3B and 4). Median coefficients are slightly positive from about sunset until sunrise, then negative through the day, which suggests that EOF 2 is dominated by up-slope flows on both flanks of the Salt Lake Valley during that time.

4.4 *Other influences*

Corollary meteorological information from the VTMX 2000 campaign allow us to explain the outliers in Fig 7A, and see why the coefficients are of unusually large magnitude. The half-hourly coefficient values during IOP 9 (20-21 October 2000) are plotted in orange and blue in Figure 7. The vertical green bar in the figure marks the approximate time of passage of a cold front across the Salt Lake Valley. University of Utah weather logs for the period state that, “A short wave trough was approaching rapidly from the west . . . Local circulations were interrupted by cold frontal passage in the valley. . .” at about 0500 LST. This cold front passage is well marked by the sudden change in the EOF 1 coefficient from large positive to large negative values, indicative of a change from strong southerly (Figure 4, green arrows) to strong northerly winds. In this case the positive values represented the southerly flow ahead of the front and subsequent negative values were caused by the flow reversal following the frontal passage. The contribution of the second EOF is small throughout the period, although the small spike may mark the passage of the front through the middle of the area. At this time there would be northerlies behind the front in the northern parts of the domain, with southerlies to the south.

5. Discussion

Several conclusions can be drawn. First, EOF analysis can identify recurring regional flow patterns and make it easy to deduce underlying physical processes governing them. A diurnal cycle of thermally induced flows dominates in the valleys that were studied, but the thermal effects can be overwhelmed by synoptic events that mimic the same patterns. These other mechanisms will, as here, often occur at the “wrong” time of day, so they can be easily recognized. Other common patterns that could be detected by EOF analysis include sea breeze cycles and features like large eddies.

EOFs provide succinct and objective characterizations of larger data sets. We have examined flow patterns (vector fields), but mixed parameter data sets can also be used if care is taken to ensure that units have fluctuations of comparable magnitude. Standard deviations are often used to standardize the data and to provide non-dimensional parameters of comparable magnitude. Once data have been described with fewer variables, it becomes possible to categorize and select specific examples of different types of atmospheric behavior for further modeling or analysis. Resources are often too limited to model very many days, so cases must be selected to represent the most important possibilities. EOF analysis is valuable for this purpose.

Acknowledgements. The work was supported by the U.S. Department of Energy under the auspices of the Atmospheric Sciences Program of the Office of Biological and Environmental Research; Organizations responsible for mesonet data that we used are: NOAA, University of Utah’s Cooperative Institute for Regional

Prediction, and the Salt Lake City NWS Forecast Office. We are grateful to the VTMX participants who provided their data, Argonne, Livermore, Los Alamos and Pacific Northwest National Laboratories, Arizona State University, University of Utah, NCAR, NOAA and others. We also acknowledge Jebb Stewart and Xindi Bian for efforts in gathering and classifying the MesoWest data that were used.

References

Doran, J. C., J. D. Fast, and J. Horel, 2002: The VTMX 2000 campaign, *Bull. Amer. Meteor. Soc.*, **83**, 537–551.

Hardy, D. M., 1977: Empirical eigenvector analysis of vector observations, *Geophys. Res. Letters*, **4**, 319-320.

Horel, J., M. Splitt, L. Dunn, J. Pechmann, B. White, C. Ciliberti, S. Lazarus, J. Slemmer, D. Zaff, and J. Burks, 2002: MesoWest: cooperative mesonets in the Western United States. *Bull. Amer. Meteor. Soc.*, **83**, 211-226.

Kaihatu, J. M., R. A. Handler, G. O. Marmorino, and L. K. Shay, 1998: Empirical orthogonal function analysis of ocean surface currents using complex and real-vector methods, *J. Atmos. and Oceanic Tech.*, **15**, 927-941

Lorenz, E. N., 1956: Empirical Orthogonal Functions and Statistical Weather Prediction, Scientific Report 1, Statistical Forecasting Project, Mass. Inst. Tech., Cambridge, Mass. (Defense Doc. Center No. 110268), 49 pp.

Ludwig, F. L., and G. Byrd, 1980: A very efficient method for deriving mass consistent flow fields from wind observations in rough terrain, *Atmos. Environ.*, **14**, 585-587.

————, J. Horel, and C. D. Whiteman, 2004: Using EOF analysis to identify important surface wind patterns in mountain valleys, *J. Appl. Meteor.*, in press.

————, J. M. Livingston, and R. M. Endlich, 1991: Use of mass conservation and dividing streamline concepts for efficient objective analysis of winds in complex terrain, *J. Appl. Meteor.*, **30**, 1490-1499.

————, R. Street, and Y. Chen, 2002: Detection and interpretation of patterns of motion in mesoscale atmospheric flows, Amer. Geophys. Union Fall Meeting and Abstracts CD, A51C-0068.

Lumley, J. L., 1981: Coherent Structures in Turbulence, *Transition and Turbulence* (R. E. Meyer, ed.), Academic Press, New York, 215-242.

Stewart, J. Q., C. D. Whiteman, W. J. Steenburgh, and X. Bian, 2002: A climatological study of thermally driven wind systems of the U. S. Intermountain West, *Bull. Amer. Meteor. Soc.*, **83**, 699-708.

Velleman, P. F., 1997: Data Desk Version 6.0 Handbook 2, Data Description, Inc., Ithaca NY, 356 pp.

von Storch, H., and F. W. Zwiers, 1999: Statistical analysis in climate research, Cambridge University Press, Cambridge, 484 pp.

Whiteman, C. D., X. Bian, and J. L. Sutherland, 1999: Wintertime surface wind patterns in the Colorado River valley. *J. Appl. Meteor.*, **38,** 1118–1130.

Wilks, D. S. , 1995: *Statistical methods in the atmospheric sciences : An introduction,* Academic Press, 467 pp.